nature geoscience

ARTICLES

PUBLISHED ONLINE: 13 MARCH 2017 | DOI: 10.1038/NGEO2914

A lower limit to atmospheric CO_2 concentrations over the past 800,000 years

E. D. Galbraith[1,2,3]* and S. Eggleston[2]

Global temperatures and atmospheric CO_2 concentrations varied widely over the glacial cycles of the past 800,000 years. But despite this variability, Antarctic ice cores have shown that CO_2 concentrations were very similar during all the coldest points of these cycles. Remarkably, the recurring minimum CO_2 concentrations (190 ± 7 ppm) fall on the lower bound of any known in Earth history. Here we show that although the volume of terrestrial ice sheets was normally distributed over the past 800,000 years, as might be expected from the approximately normal distribution of the orbital forcing that drove the glacial cycles, Antarctic temperatures have a strong cold mode, whereas CO_2 concentrations have both a cold mode and a central mode. Although multiple explanations are possible, the recurring CO_2 minima and pronounced cold modes are consistent with a strong negative feedback to decreasing CO_2 that resisted further cooling on timescales shorter than 10,000 years. We suggest that one possible negative feedback is CO_2-limitation of photosynthesis, either directly or via CO_2-limitation of N_2 fixation, which could have inhibited further lowering of CO_2 by reducing carbon storage.

For decades, investigators have sought a simple, unifying mechanism to explain the observed correlation of atmospheric CO_2 and temperature in Antarctic ice cores over the glacial cycles. In general, these explanations call on a shift in the partitioning of carbon between the ocean and atmosphere[1], accounting for a small change in the terrestrial biosphere but no other change in the size of the carbon inventory[2–4]. However, there is now a growing realization that the ocean–atmosphere carbon inventory could have varied more significantly[5], due to isostasy-driven changes in CO_2 outgassing rates[6–8], changes in permafrost and peatlands[9], and variations in marine carbon burial[10]. The importance of geological changes in the carbon inventory chips away at the ability of a single unified mechanism to explain the history of CO_2 over glacial cycles. Rather, it would appear that the CO_2 history was actually the product of a complex chain of events involving many players, including ocean circulation, the marine ecosystem, the terrestrial biosphere, and interactions between ice sheets and the lithosphere.

Given this apparent complexity, one feature of the Antarctic ice-core records, which has previously received little attention, takes on new significance. As shown in Fig. 1, although each of the past 8 glacial cycles had its own peculiarities, the minima of δD (a proxy for Antarctic atmospheric temperature) and CO_2 were always very similar: -440 ± 5‰ and 190 ± 7 ppm, respectively. This similarity contrasts sharply with the interglacials, during which δD and CO_2 varied more broadly (Supplementary Table 1). It also contrasts with the different temporal pathways followed by δD and CO_2; although their overall correlation is striking, they diverge from a linear relationship over periods spanning many thousands of years.

The CO_2 minima are also remarkable when compared with reconstructions of atmospheric CO_2 before the ice ages[11,12]. Although CO_2 has often been far higher than during interglacials, exceeding 1,000 ppm (ref. 13), there are no reconstructions showing unambiguously lower values than the glacial CO_2 minima. In fact, a recent reconstruction of atmospheric CO_2 during the last prolonged 'icehouse' of the Carboniferous period shows that minimum values of ~200 ppm were repeatedly reached during Carboniferous glaciations, indistinguishable (within uncertainty) from the minima recorded in ice cores spanning the past 800 kyr (ref. 14). Together,

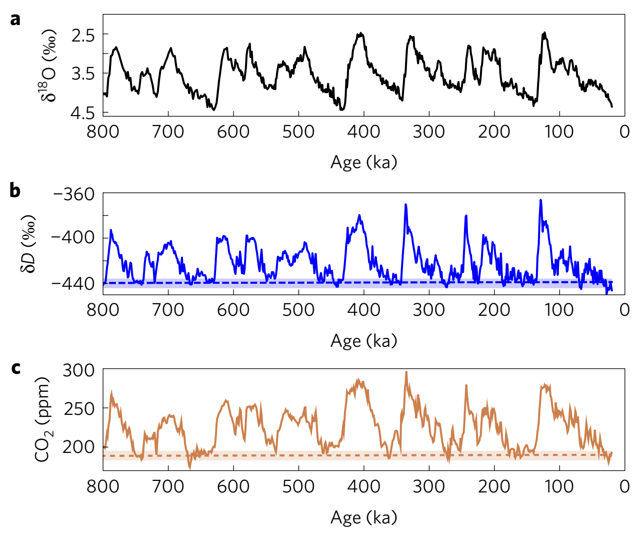

Figure 1 | Glacial cycles over the past 800 kyr. a–c, Time-series curves showing a global stack of benthic foraminifera $\delta^{18}O$ (ref. 48) (**a**), the EPICA Dome C ice-core δD record[49] (**b**), and a compilation of atmospheric CO_2 records from multiple ice cores[45] (**c**) over the period 800–20 ka. The horizontal dashed lines indicate the average minima of δD and CO_2; shading shows 1 s.d. around these minima. The minima of $\delta^{18}O$, which reflect a combination of terrestrial ice volume and deep sea temperature, are more variable and therefore not indicated.

[1]ICREA, Pg. Lluís Companys 23, 08010 Barcelona, Spain. [2]Institut de Ciència i Tecnologia Ambientals (ICTA) and Department of Mathematics, Universitat Autònoma de Barcelona, 08193 Barcelona, Spain. [3]Department of Earth and Planetary Science, McGill University, Montreal, Quebec H3A 2A7, Canada. *e-mail: eric.galbraith@icrea.cat

these observations raise an important question: is there a lower limit to atmospheric CO_2 on the geologically short timescale of glacial cycles?

Statistical analysis

We first take a closer look at the features of the Antarctic ice-core δ*D* and CO_2 records, in comparison with the calculated peak summertime insolation at 65° N, and a reconstruction of the global volume of terrestrial ice (expressed as relative sea level). For the latter, we use the stacked benthic foraminifera-derived estimates given by ref. 15, but alternative reconstructions yield similar results (Supplementary Figs 1 and 2). For all, we use the time period 800–20 thousand years ago (ka), which begins and ends just before deglaciations.

Figure 2 shows the frequency distributions of the four time series. Like the orbitally determined insolation (Fig. 2a), the sea level reconstructions follow a normal distribution (Fig. 2b), with a clear mode of −31 m that is close to the mean value of −37 m. In contrast, the Antarctic δ*D* has a single mode that is strongly skewed to cold values (Fig. 2c). In fact, the most common Antarctic δ*D* is very close to the lowest recorded Antarctic δ*D*, showing a clear preference for the cold state. A global air surface temperature (GAST) reconstruction[16] also shows a cold mode, although with considerably less skew, as shown in Supplementary Figs 3–5. The greater skew of δ*D* relative to the GAST reconstruction could reflect nonlinear impacts of Southern Ocean sea ice and atmospheric circulation at the Antarctic ice-core site (see Supplementary Discussion 2). In addition, we note that the GAST reconstruction does not show the consistent lower bound observed for δ*D* (Supplementary Fig. 4). We are not aware whether this absence indicates that the lower bound of temperature (Fig. 1b) is specific to Antarctica, or if it reflects uncertainty in the GAST reconstruction. Regardless, the apparent preference for the cold state is a remarkable contrast with the rarity of maximum ice-sheet volume.

Figure 2d shows that CO_2 has a more complex frequency distribution, with two clear modes near 200 and 240 ppm that could perhaps correspond to the low mode of Antarctic δ*D* and the central mode of ice volume, respectively. The CO_2 distribution is notably less-skewed than that of Antarctic δ*D*, and is of similar skewness to the GAST reconstruction. A third mode, which is much weaker but nonetheless significant, occurs at the interglacial CO_2 of 275 ppm over the past four glacial cycles but was absent during the lukewarm interglacial cycles (800–440 ka) when both CO_2 and Antarctic δ*D* were more normally distributed (Supplementary Figs 6 and 7). But despite differences between the earlier and later cycles, the lower bounds of atmospheric CO_2 and Antarctic δ*D* were very similar, and the low CO_2 and δ*D* modes remained pronounced throughout the past 800 kyr.

The fact that ice sheets were very rarely at their largest extents, despite the preference of CO_2 and Antarctic temperature for the cold states, is consistent with direct orbital forcing and internal ice-sheet dynamics having exerted strong controls on ice-sheet size[17]. We focus now on potential mechanisms to explain the Earth system preference for a relatively invariant, cold, low-CO_2 state.

Possible stabilizing feedback pathways

A lower bound on Antarctic temperature and CO_2 could be explained by an instability threshold, by which arrival at the coldest state triggers rapid warming[18,19]. However, a direct trigger cannot explain the preference for the cold state, and is inconsistent with the heterogeneous durations of the coldest periods (Supplementary Table 2). Instead, we hypothesize that the coldest, lowest-CO_2 states were the most common over the past 800 kyr because of one or more stabilizing feedbacks that resisted further cooling, on a timescale of <10 kyr. As such, any cooling tendency would have encountered increasing resistance as the temperature fell, leading to a preferred state.

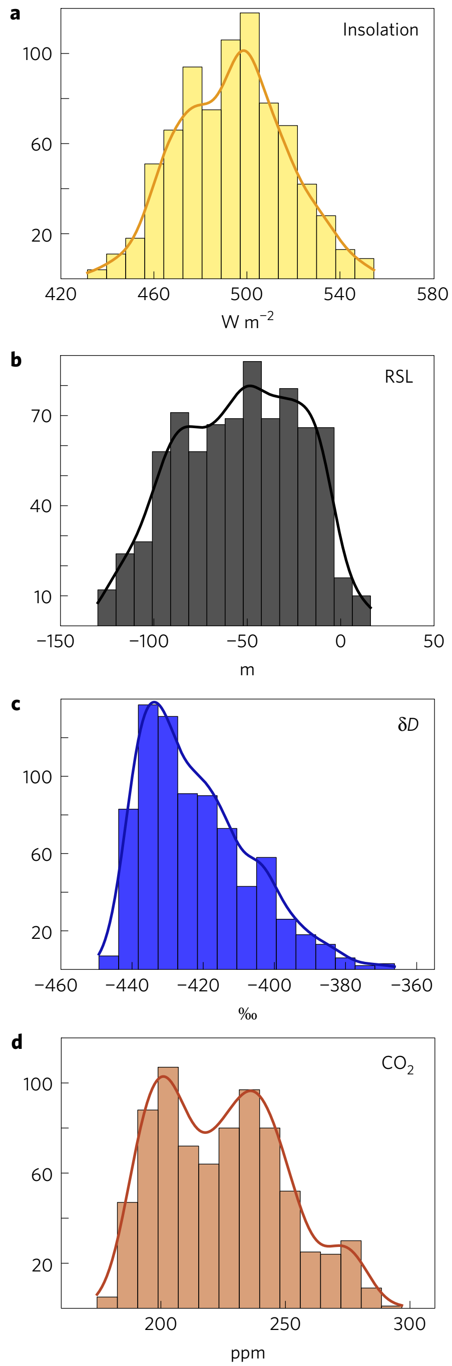

Figure 2 | Frequency distributions of insolation, sea level, Antarctic temperature and CO_2 over glacial cycles. a–d, Histograms showing the frequency of occurrence of 21 June insolation at 65° N (**a**), relative sea level[15] (**b**), the EPICA Dome C ice-core δ*D* (ref. 49) (**c**), and atmospheric CO_2 (ref. 45) (**d**) over the period 800–20 ka. The frequency distributions are calculated from 1-kyr interpolated time series and are shown on the vertical axes, both for discrete bins and as smooth distributions using the MATLAB ksdensity function.

The lower bounds and cold modes of δ*D* and CO_2 suggest that one or more stabilizing feedbacks affected CO_2 and/or Antarctic temperature. But because Antarctic temperature is related to global temperature, which is coupled to CO_2, it is not clear whether the feedback(s) acted on just one of the two, on both, or on the coupling

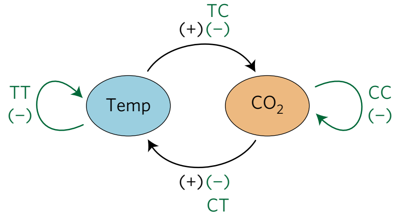

Figure 3 | Schematic illustration of feedbacks acting on temperature and atmospheric CO_2. The black arrows indicate positive feedbacks, representing the radiative effect of CO_2 on global atmospheric temperature (Temp), and any mechanisms by which lower global temperatures lead to reduced CO_2, such as the temperature-dependent solubility of CO_2 in seawater. The green arrows indicate conceivable negative feedbacks acting on temperature, CO_2, or the coupling between them. The negative feedbacks are labelled here according to the variable that causes the feedback (temperature, 'T' or CO_2, 'C') followed by the variable on which the feedback would act. For example, feedback TC would involve a decrease of temperature that produced an increase of atmospheric CO_2.

between them (Fig. 3). We therefore consider four non-exclusive pathways by which negative feedbacks may have operated.

First, the lower limit could have been maintained by a temperature-controlled negative feedback, which resisted further cooling at low temperatures (TT). One such physical limit is the freezing point of seawater: waters feeding the deep ocean cannot be cooled below $-2\,^{\circ}C$, a limit that was closely approached during the glacial maximum (LGM)[20]. However, the temperature of the deep ocean has little effect on the global atmosphere, since the outcrop regions of deep waters represent a very small fraction of the Earth surface. In addition, we are unaware of any such limit in climate models, which continue to cool as CO_2 is lowered below 180 ppm. A second possible feedback pathway, by which the CO_2 impact on temperature is reduced in the cold state (CT), is also in conflict with the tendency of climate models to show an increasing sensitivity to radiative forcing as the climate cools[21]. Thus, pathways TT and CT both appear unlikely.

A third pathway involves physical mechanisms that could prevent further lowering of CO_2 as the Earth grows very cold (TC). For example, it has been speculated that more extensive sea ice in the Southern Ocean reduced atmospheric CO_2 during ice ages, due to both its effect on ocean circulation[22] and direct impedance of outgassing[23–25]. A limit to the extent of Southern Ocean sea ice, or to its impact on carbon storage via ocean circulation or air–sea exchange, could have prevented CO_2 from decreasing further, and a role of the Southern Ocean in limiting CO_2 drawdown would be intuitively consistent with the consistent lower bound and strong skew of Antarctic δD. However, if such a temperature-sensitive feedback acts exclusively on the air–sea partitioning of CO_2, it would not have been sensitive to changes in the combined air–sea carbon inventory. Thus, if changes in the terrestrial biosphere or geological processes had produced a significant contrast in the ocean–atmosphere carbon pool between CO_2 minima, it would have led to different atmospheric CO_2 for the same air–sea partitioning. This prediction suggests a means by which the TC pathway could be tested in future.

In addition, the TC pathway cannot obviously explain the similar CO_2 minima during the Carboniferous ice ages[14], and would raise the question why it did not prevent 'snowball' episodes from occurring in the more distant past. It has been well documented that large ice sheets invaded the low latitudes multiple times during the Neoproterozoic era[26]. Intriguingly, CO_2 levels could have been significantly higher during Neoproterozoic snowball initiation than during the LGM[27] because the relative faintness of the Sun would have allowed glaciation to occur at significantly higher CO_2 levels. Although highly speculative, this would tentatively point towards a feedback that is sensitive to the CO_2 concentration itself.

This leads to the final pathway, CC, which would either increase the ocean–atmosphere C inventory or shift C from the ocean to the atmosphere, in response to falling CO_2. Silicate weathering rates are thought to decrease as terrestrial temperatures and precipitation decrease, which would lead to an increase in the C inventory, stabilizing atmospheric CO_2 on a $>10^5$ yr timescale[28,29], but the reaction time would appear to be too slow to provide a strong control on the $<10^4$ yr timescale of the glacial CO_2 minima[30]. An alternative is the dependence of photosynthetic organisms on CO_2.

CO_2-limitation of photosynthesis

In terrestrial ecosystems, carbon fixation by plants is limited by low ambient CO_2 (ref. 31). On this basis, ref. 12 proposed that CO_2-limitation had significantly reduced plant-mediated silicate weathering during low-CO_2 intervals of the past 24 million years, thereby enforcing a lower bound on the ocean–atmosphere carbon inventory over $>10^5$ yr timescales. Subsequent experiments have been consistent with this 'carbon starvation' mechanism, showing reduced weathering by tree-root-associated fungi under low CO_2 (ref. 32). Although the feedback on silicate weathering would appear too slow to play a role on the 10^4 yr timescale of glacial CO_2 minima[30], it may be possible that strongly reduced weathering rates lowered ocean alkalinity (thereby decreasing CO_2 solubility) on a millennial timescale. Alternatively, reduced photosynthesis rates during the LGM would have slowed the accumulation of terrestrial biomass[14], consistent with estimates for lower terrestrial primary production rates[33]. By slowing the accumulation of carbon in vegetation and soils, this would have provided a stabilizing feedback via an increase of the ocean–atmosphere carbon pool.

Finally, in the ocean, CO_2-limitation can reduce growth rates among some phytoplankton taxa[34]. Laboratory experiments have suggested that marine N_2 fixing cyanobacteria are especially sensitive to low CO_2 (ref. 35), with growth rates strongly decreased below a p_{CO_2} of 200 ppm (ref. 36). N_2 fixers play a critical role in the marine ecosystem, counteracting the continual loss of fixed nitrogen by denitrification. This biologically available nitrogen is the primary limiting nutrient for the export of organic matter, which is responsible for the ocean biological 'soft tissue' carbon pump[37]. Marine sediment records have suggested that the global soft tissue pump was stronger during the LGM than during the Holocene[38], but at the same time, N_2 fixation rates appear to have been much slower than during the Holocene[39,40], which has been commonly attributed to reduced phosphorus availability given slower rates of denitrification[41] despite more abundant Fe supply from dust[42,43]. If N_2 fixation had also been progressively handicapped as CO_2 fell because N_2 fixers were having a hard time growing, it could have put the brakes on the strengthening of the soft tissue pump, shifting carbon from the ocean back to the atmosphere as CO_2 fell to very low values.

The analysis here highlights the consistency of CO_2 minima, and the strong low mode of CO_2, as unexplained aspects of late Pleistocene glacial cycles. The proposed lower bound on CO_2 could have implications for understanding the periodicity of glacial cycles[44], as well as the constancy of average CO_2 over the past 800 kyr (ref. 28). Although our discussion points towards a CO_2-stabilizing feedback that responds directly to the CO_2 concentration itself, we cannot currently provide a definitive test of the proposed hypotheses given a lack of suitable observational constraints, and additional hypotheses are entirely possible. Notably, Fig. 1 shows one brief excursion of CO_2 below the typical glacial minimum at $\sim$667 ka, when EPICA Dome C ice-core measurements reach a minimum of 174 ppm (refs 45,46). The absolute value of this minimum should be regarded with care, as specific measurement methods in technically challenging sections of the ice core can also lead to erroneous results[46,47]. However, if real, its brevity (a few thousand years) could indicate the timescale on which the negative feedback operates, and further study of this time interval might help to test possible mechanisms regarding what appears to be a fundamental, yet unexplained, homeostatic regulation of the Earth system.

Methods

Methods, including statements of data availability and any associated accession codes and references, are available in the online version of this paper.

Received 18 October 2016; accepted 15 February 2017; published online 13 March 2017

References

1. Broecker, W. S. & Denton, G. H. The role of ocean–atmosphere reorganizations in glacial cycles. *Geochim. Cosmochim. Acta* **53,** 2465–2501 (1989).
2. Jaccard, S. L. *et al*. Two modes of change in Southern Ocean productivity over the past million years. *Science* **339,** 1419–1423 (2013).
3. Sigman, D. M. & Boyle, E. A. Glacial/interglacial variations in atmospheric carbon dioxide. *Nature* **407,** 859–869 (2000).
4. Sigman, D. M., Hain, M. P. & Haug, G. H. The polar ocean and glacial cycles in atmospheric CO_2 concentration. *Nature* **466,** 47–55 (2010).
5. Broecker, W. S., Yu, J. & Putnam, A. E. Two contributors to the glacial CO_2 decline. *Earth Planet. Sci. Lett.* **429,** 191–196 (2015).
6. Huybers, P. & Langmuir, C. Feedback between deglaciation, volcanism, and atmospheric CO_2. *Earth Planet. Sci. Lett.* **286,** 479–491 (2009).
7. Lund, D. C. *et al*. Enhanced East Pacific Rise hydrothermal activity during the last two glacial terminations. *Science* **351,** 478–482 (2016).
8. Ronge, T. A. *et al*. Radiocarbon constraints on the extent and evolution of the South Pacific glacial carbon pool. *Nat. Commun.* **7,** 11487 (2016).
9. Zech, R. A permafrost glacial hypothesis—permafrost carbon might help explaining the Pleistocene ice ages. *Quat. Sci. J.* **61,** 84–92 (2012).
10. Cartapanis, O., Bianchi, D., Jaccard, S. L. & Galbraith, E. D. Global pulses of organic carbon burial in deep-sea sediments during glacial maxima. *Nat. Commun.* **7,** 10796 (2016).
11. Royer, D. L. in *Treatise on Geochemistry* Vol. 6, 2nd edn, 251–267 (Elsevier, 2014).
12. Pagani, M., Caldeira, K., Berner, R. & Beerling, D. J. The role of terrestrial plants in limiting atmospheric CO_2 decline over the past 24 million years. *Nature* **460,** 85–88 (2009).
13. Anagnostou, E. *et al*. Changing atmospheric CO_2 concentration was the primary driver of early Cenozoic climate. *Nature* **533,** 380–384 (2016).
14. Montañez, I. P. *et al*. Climate, p_{CO_2} and terrestrial carbon cycle linkages during late Palaeozoic glacial–interglacial cycles. *Nat. Geosci.* **9,** 824–828 (2016).
15. Spratt, R. M. & Lisiecki, L. E. A late Pleistocene sea level stack. *Clim. Past* **12,** 1079–1092 (2016).
16. Snyder, C. W. Evolution of global temperature over the past two million years. *Nature* **538,** 226–228 (2016).
17. Abe-Ouchi, A. *et al*. Insolation-driven 100,000-year glacial cycles and hysteresis of ice-sheet volume. *Nature* **500,** 190–193 (2013).
18. Paillard, D. & Parrenin, F. The Antarctic ice sheet and the triggering of deglaciations. *Earth Planet. Sci. Lett.* **227,** 263–271 (2004).
19. Gildor, H. & Tziperman, E. A sea ice climate switch mechanism for the 100-kyr glacial cycles. *J. Geophys. Res.* **106,** 9117–9133 (2001).
20. Adkins, J. F., McIntyre, K. & Schrag, D. P. The salinity, temperature, and $\delta^{18}O$ of the glacial deep ocean. *Science* **298,** 1769–1773 (2002).
21. Manabe, S. & Bryan, K. CO_2-induced change in a coupled ocean–atmosphere model and its paleoclimatic implications. *J. Geophys. Res.* **90,** 11689–11707 (1985).
22. Ferrari, R. *et al*. Antarctic sea ice control on ocean circulation in present and glacial climates. *Proc. Natl Acad. Sci. USA* **111,** 8753–8758 (2014).
23. Stephens, B. B. & Keeling, R. F. The influence of Antarctic sea ice on glacial–interglacial CO_2 variations. *Nature* **404,** 171–174 (2000).
24. Brovkin, V., Ganopolski, A., Archer, D. & Munhoven, G. Glacial CO_2 cycle as a succession of key physical and biogeochemical processes. *Clim. Past* **8,** 251–264 (2012).
25. Gildor, H., Tziperman, E. & Toggweiler, J. R. Sea ice switch mechanism and glacial-interglacial CO_2 variations. *Glob. Biogeochem. Cycles* **16,** 3 (2002).
26. Hoffman, P. F., Kaufman, A. J., Halverson, G. P. & Schrag, D. P. A neoproterozoic snowball earth. *Science* **281,** 1342–1346 (1998).
27. Pierrehumbert, R. T., Abbot, D. S., Voigt, A. & Koll, D. Climate of the neoproterozoic. *Annu. Rev. Earth Planet. Sci.* **39,** 417–460 (2011).
28. Zeebe, R. E. & Caldeira, K. Close mass balance of long-term carbon fluxes from ice-core CO_2 and ocean chemistry records. *Nat. Geosci.* **1,** 312–315 (2008).
29. Kump, L. R., Brantley, S. L. & Arthur, M. A. Chemical weathering, atmospheric CO_2, and climate. *Annu. Rev. Earth Planet. Sci.* **28,** 611–667 (2000).
30. Ridgwell, A. & Hargreaves, J. Regulation of atmospheric CO_2 by deep-sea sediments in an Earth system model. *Glob. Biogeochem. Cycles* **21,** GB2008 (2007).
31. Ehleringer, J. R., Cerling, T. E. & Helliker, B. R. C_4 photosynthesis, atmospheric CO_2, and climate. *Oecologia* **112,** 285–299 (1997).
32. Quirk, J., Leake, J. R., Banwart, S. A., Taylor, L. L. & Beerling, D. J. Weathering by tree-root-associating fungi diminishes under simulated Cenozoic atmospheric CO_2 decline. *Biogeosciences* **11,** 321–331 (2014).
33. Ciais, P. *et al*. Large inert carbon pool in the terrestrial biosphere during the last glacial maximum. *Nat. Geosci.* **5,** 74–79 (2012).
34. Riebesell, U. & Tortell, P. D. in *Ocean Acidification* (eds Gattuso, J.-P. & Hansson, L.) 99–121 (Oxford Univ. Press, 2011).
35. Hutchins, D. A. *et al*. CO_2 control of *Trichodesmium* N_2 fixation, photosynthesis, growth rates, and elemental ratios: implications for past, present, and future ocean biogeochemistry. *Limnol. Oceanogr.* **52,** 1293–1304 (2007).
36. Hutchins, D. A., Fu, F.-X., Webb, E. A., Walworth, N. & Tagliabue, A. Taxon-specific response of marine nitrogen fixers to elevated carbon dioxide concentrations. *Nat. Geosci.* **6,** 790–795 (2013).
37. Moore, C. M. *et al*. Processes and patterns of oceanic nutrient limitation. *Nat. Geosci.* **6,** 701–710 (2013).
38. Galbraith, E. D. & Jaccard, S. L. Deglacial weakening of the oceanic soft tissue pump: global constraints from sedimentary nitrogen isotopes and oxygenation proxies. *Quat. Sci. Rev.* **109,** 38–48 (2015).
39. Galbraith, E. D. *et al*. The acceleration of oceanic denitrification during deglacial warming. *Nat. Geosci.* **6,** 579–584 (2013).
40. Ren, H. *et al*. Foraminiferal isotope evidence of reduced nitrogen fixation in the ice age Atlantic Ocean. *Science* **323,** 244–248 (2009).
41. Ganeshram, R. S., Pedersen, T. F., Calvert, S. & François, R. Reduced nitrogen fixation in the glacial ocean inferred from changes in marine nitrogen and phosphorus inventories. *Nature* **415,** 156–159 (2002).
42. Falkowski, P. G. Evolution of the nitrogen cycle and its influence on the biological sequestration of CO_2 in the ocean. *Nature* **387,** 272–275 (1997).
43. Eugster, O., Gruber, N., Deutsch, C., Jaccard, S. L. & Payne, M. R. The dynamics of the marine nitrogen cycle across the last deglaciation. *Paleoceanography* **28,** 116–129 (2013).
44. Crucifix, M. Oscillators and relaxation phenomena in Pleistocene climate theory. *Phil. Trans. R. Soc. A* **370,** 1140–1165 (2012).
45. Lüthi, D. *et al*. High-resolution carbon dioxide concentration record 650,000–800,000 years before present. *Nature* **453,** 379–382 (2008).
46. Bereiter, B. *et al*. Revision of the EPICA Dome C CO_2 record from 800 to 600 kyr before present. *Geophys. Res. Lett.* **42,** 542–549 (2015).
47. Bereiter, B. *et al*. Mode change of millennial CO_2 variability during the last glacial cycle associated with a bipolar marine carbon seesaw. *Proc. Natl Acad. Sci. USA* **109,** 9755–9760 (2012).
48. Lisiecki, L. E. & Raymo, M. E. A Pliocene-Pleistocene stack of 57 globally distributed benthic $\delta^{18}O$ records. *Paleoceanography* **20,** PA1003 (2005).
49. Jouzel, J. *et al*. Orbital and millennial Antarctic climate variability over the past 800,000 years. *Science* **317,** 793–796 (2007).

Acknowledgements

We thank S. Jaccard, D. Hutchins and members of the CIFAR Earth System Evolution Program for helpful discussions. E. Wolff, C. Pelejero, E. Calvo and S. Hall provided constructive comments on the manuscript. Financial support was provided by the Spanish Ministry of Economy and Competitiveness through the María de Maeztu Programme for Centres of Excellence in R&D (MDM-2015-0552), and the Swiss National Science Foundation through an Early Postdoc.Mobility grant.

Author contributions

E.D.G. initiated the study and wrote the first draft of the paper. S.E. contributed to the development of figures, analysis and revisions of the text.

Additional information

Supplementary information is available in the online version of the paper. Reprints and permissions information is available online at www.nature.com/reprints. Publisher's note: Springer Nature remains neutral with regard to jurisdictional claims in published maps and institutional affiliations. Correspondence and requests for materials should be addressed to E.D.G.

Competing financial interests

The authors declare no competing financial interests.

Methods

Data availability. The data used in this paper are available at the following sources.

Bereiter *et al.* (2015), CO_2 data: http://onlinelibrary.wiley.com/store/10.1002/2014GL061957/asset/supinfo/grl52461-sup-0003-supplementary.xls?v=1&s=e77ad89c3925111330671009ab40eac65e019d01.

Snyder (2016), GAST reconstruction: http://www.nature.com/nature/journal/v538/n7624/extref/nature19798-s2.xlsx.

Lisiecki and Raymo (2005), $\delta^{18}O$ stack: ftp://ftp.ncdc.noaa.gov/pub/data/paleo/contributions_by_author/lisiecki2005/lisiecki2005.txt.

Spratt and Lisiecki (2016), RSL reconstruction: http://www.clim-past.net/12/1079/2016/cp-12-1079-2016-supplement.pdf.

Elderfield *et al.* (2012), RSL reconstruction: https://doi.pangaea.de/10.1594/PANGAEA.786204

Shakun *et al.* (2015), RSL reconstruction: http://www.sciencedirect.com/science/MiamiMultiMediaURL/1-s2.0-S0012821X15003404/1-s2.0-S0012821X15003404-mmc2.xlsx/271830/html/S0012821X15003404/f6d10775fdb9a93592ba44ffc931547a/mmc2.xlsx.

Jouzel *et al.* (2007), δD data and Antarctic temperature reconstruction: https://doi.pangaea.de/10.1594/PANGAEA.683655.

Bazin *et al.* (2013), updated age scale for EDC: https://doi.pangaea.de/10.1594/PANGAEA.824865.

nature geoscience | SUPPLEMENTARY INFORMATION
DOI: 10.1038/NGEO2914
In the format provided by the authors and unedited.

A lower limit to atmospheric CO_2 concentrations over the past 800,000 years

Eric D. Galbraith and Sarah Eggleston

Supplementary Discussion

SD1. Possible limits of CO_2 detection or preservation in ice cores

Any bias in preservation or measurement at low CO_2 concentrations would potentially influence the statistical distribution of CO_2 over time. We therefore review the measurement techniques and possible preservation issues in detail.

All of the CO_2 measurement studies presented here use a dry mechanical extraction technique[1-5] with the exception of one, which employs the use of sublimation extraction[6]. The mechanical extraction typically involves insertion of the ice sample into a chamber under high vacuum and crushing of the ice using needles to pulverize the ice and allow the entrapped gas to be released. In the latter technique, the sample is sublimated under vacuum to release the air from the bubbles and clathrates with 100% efficiency. In all methods, CO_2 (often together with N_2O) is separated from the other gases, and the concentration is measured using gas chromatography.

Several issues must be considered when translating the measured CO_2 into atmospheric CO_2 values of the past. While the typical analytical measurement precision is approximately 1 ppm for modern measurement systems, the procedure may produce a non-zero “blank,” determined by passing a standard gas of known CO_2 concentration over gas-free ice. The “blank” may be as high as 10 ppm[7]. This could be due to release or adsorption of CO_2 by the apparatus and is subtracted from the chromatography measurement. The standard gases typically have concentrations of CO_2 between 180 and 280 ppm, and while it cannot be excluded that the calibration below this range is exactly linear, “blank” measurements have been shown to produce values close to zero on a similar measurement system[8]; thus, the lower detection limit lies well below the lower bound of the data.

Within the ice core, processes have been identified that could cause production of CO_2 either due to the presence of particular inorganic[9] or organic[10] compounds. However, *in situ* production of CO_2 at least during the past two glacial periods can be excluded from Antarctic ice cores based on evidence from measurements of the stable carbon isotope during these periods[11,12]. Gravitational fractionation of gases causes CO_2 to be preferentially excluded from the firn, thus enriching the concentration in the underlying ice. However, this effect results in a correction of less than 2 ppm[13]. The mechanical extraction technique has been found to be inaccurate in regions of the ice core containing both bubbles and clathrates, perhaps due to fractionation of CO_2 between these two structures[14], but this effect is isolated to the particular depth range in each ice core where both bubbles and clathrates are found, which has been excluded from the data presented here.

It is important to interpret the absolute values of the CO_2 minima carefully, given that offsets have been noted among some ice cores on the order of 4 ppm[13,15,16], the cause of which is not yet entirely understood. However, CO_2 during six of the eight glacial periods discussed here has been measured on a single ice core (EPICA Dome C). The remaining two were measured on Dome Fuji, and the period of overlap of these two ice cores shows good agreement. Thus, while the absolute values of the data used in this study may be shown to have a slight error, this would not affect the distributions discussed here.

In summary, it appears unlikely that the low CO_2 measurements are biased to any significant degree, and are very likely robust within an absolute uncertainty of 5 ppm.

SD2. Relationship between δD, Antarctic and global temperature

We use δD as a proxy for global temperature, given that it is precisely defined, and is available at the same high sampling resolution as the CO_2 measurements, making it suitable for the statistical analyses. Here we discuss the likely bias between δD, the local Antarctic temperature, and globally-averaged surface air temperature.

While δD is primarily a function of site temperature, it depends as well on the temperature at the water vapor source[17]. Therefore, the relationship between δD measured at EDC and Antarctic temperature is not strictly linear. While deuterium excess measurements ($d = \delta D - 8\,\delta^{18}O$) allow for necessary corrections, thus providing a better estimate of Antarctic temperature, these data are only available over one glacial cycle. However, the data over this period indicate that the corrections of modeled temperature using only δD are small[18,19]. Models have shown that sea ice can have an impact on the stable water isotopes in Antarctic ice cores[20] due to changes in precipitation regions; this can be significant at coastal sites. However, the data discussed here are derived from EPICA Dome C, located far from the coast, where this effect is believed to be small. As shown in Figure S3, the frequency distribution of Antarctic temperatures, calculated from the δD, is not noticeably different than the δD distribution.

When considering the relationship between Antarctic temperature and globally-averaged surface air temperature, one would expect temperature changes in Antarctica to have been larger due to polar amplification. The temperature in Antarctica could have been additionally modified by changes in sea ice extent in the Southern Ocean, and changes in atmospheric circulation. In order to test the influence these may have had on the frequency distribution, we take advantage of the reconstruction of globally-averaged surface air temperature (GAST) provided by Ref. [21]. As shown in Figures S??, the cold mode of temperature is also evident in the global average. Intriguingly, the distribution of temperatures in the GAST reconstruction is more similar to that of CO_2 than that of δD.

Table S-1. Variability among coldest periods compared to warmest periods of the last 800 ky. The means and standard deviations (S.D.) are shown for the lowest and highest 13% of the respective 1-kyr binned datasets, 20-800 kyr. The Antarctic temperature is given as degrees C relative to the last 1000y, as derived from δD. As shown in the final column, the standard deviations of the warm periods (87-100%) are much higher than those of the cold periods.

Parameter	Mean 0-13%	S.D. 0-13%	Mean 87-100%	S.D. 87-100%	S.D. warm/cold
CO_2 (ppm)	190.0	4.0	268.0	9.9	2.4
Ant temp (^oC), δD	-8.9	0.4	0.0	1.6	3.9

Table S-2. Durations of coldest periods of the last 800 ky. Coldest periods are identified as continuous periods around local minima during which the 10-ky running mean of the respective parameter is within the given range of the local minimum. The durations are mostly on the order of 12 ky, but two are significantly longer, which is not consistent with a straightforward trigger mechanism by which cold climates initiate deglaciation.

(a) CO_2, range: 7 ppm

Minimum (ky BP)	Minimum (ppm)	Start (ky BP)	End (ky BP)	Duration (ky)
27	187.8	20	33	13
158	192.5	139	178	39
273	193.0	269	278	9
362	194.1	357	369	12
460	197.5	439	468	29
539	203.3	533	549	16
665	184.7	660	672	12
744	187.5	740	752	12

(b) δD, range: 5 ‰

Minimum (ky BP)	Minimum (‰)	Start (ky BP)	End (ky BP)	Duration (ky)
25	-444.0	21	33	12
142	-437.2	137	177	40
275	-440.2	269	281	12
358	-436.8	344	369	25
442	-439.9	434	449	15
547	-434.1	536	553	17
637	-437.9	631	647	16
746	-438.8	739	754	15

Supplementary Figures

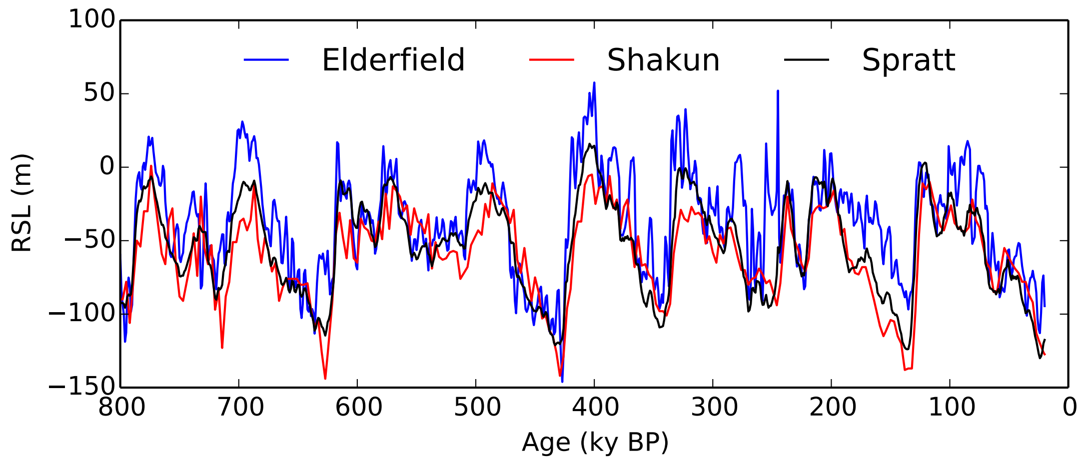

Figure S1. Comparison of three reconstructions of relative sea level [22-24] over time.

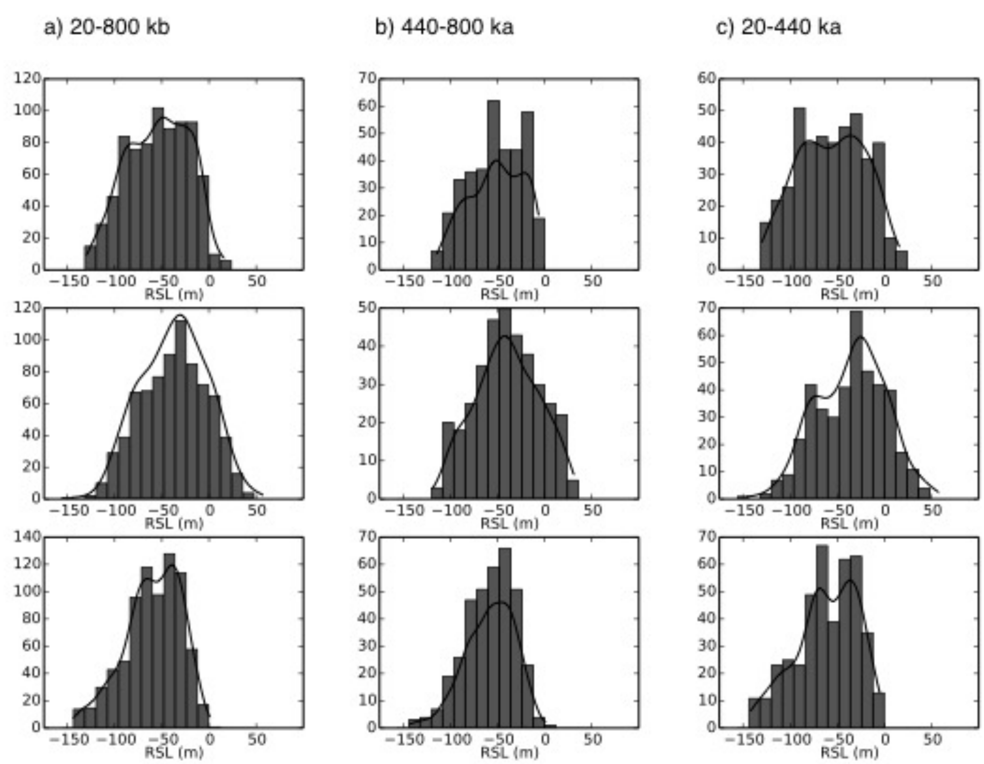

Figure S2: Histograms comparing the sea level reconstructions by ref. 24, top panels; ref. 22, middle panels; and ref. 23, bottom panels, arranged in columns according to the time periods (a) 20-800 ka (b) 440-800 ka, and (c) 20-440 ka.

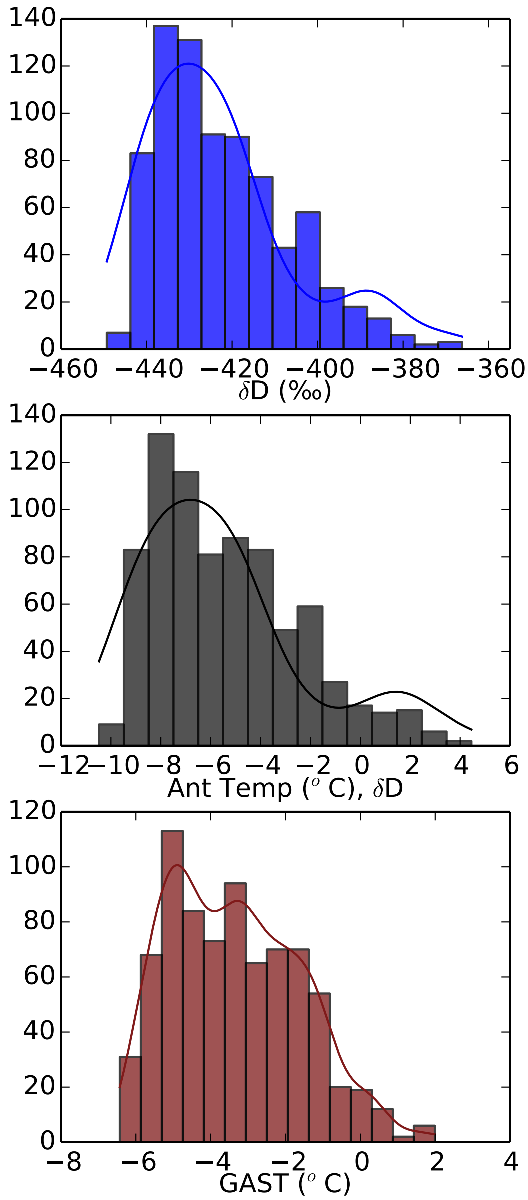

Figure S3. Antarctic δD compared to local temperature and global temperature. The top panel shows the frequency distribution for δD over the full 20-800 ka period. The middle panel shows the frequency distribution of temperatures, estimated from δD at EPICA Dome C. The lower panel shoes the Global Average Surface Temperature (GAST) reconstruction of Ref. 21.

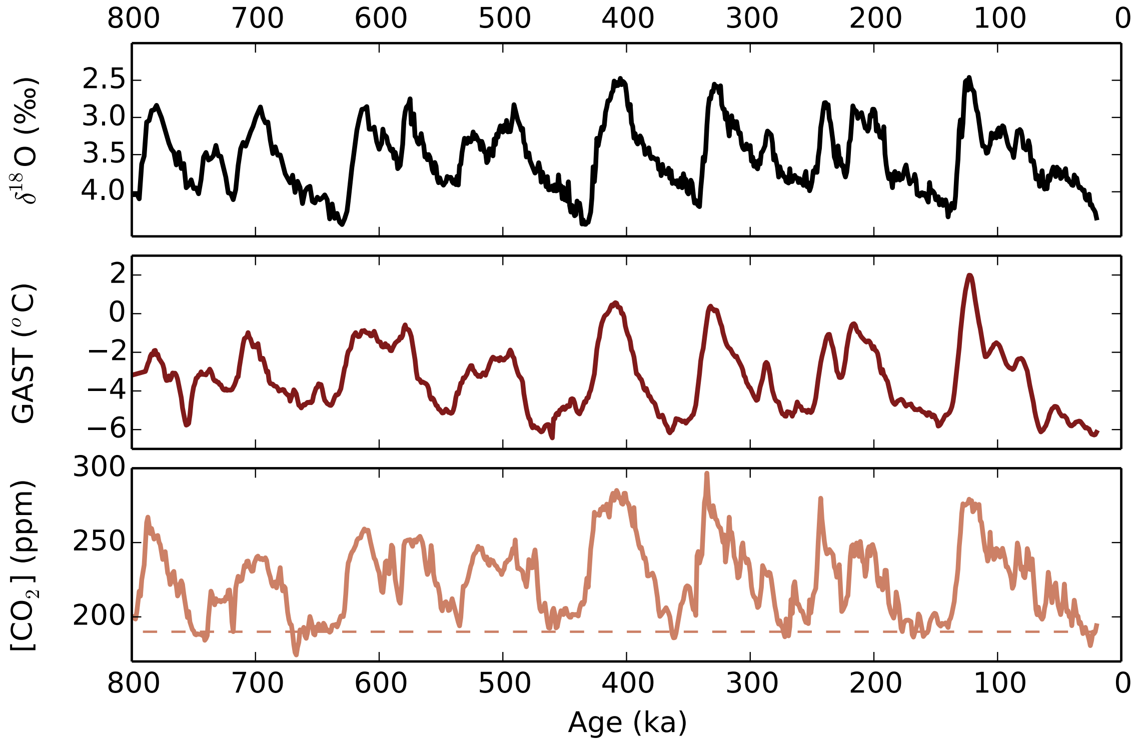

Figure S4. Timeseries using the Global Average Surface Temperature reconstruction of Ref. 21. As Figure 1, but replacing δD with GAST.

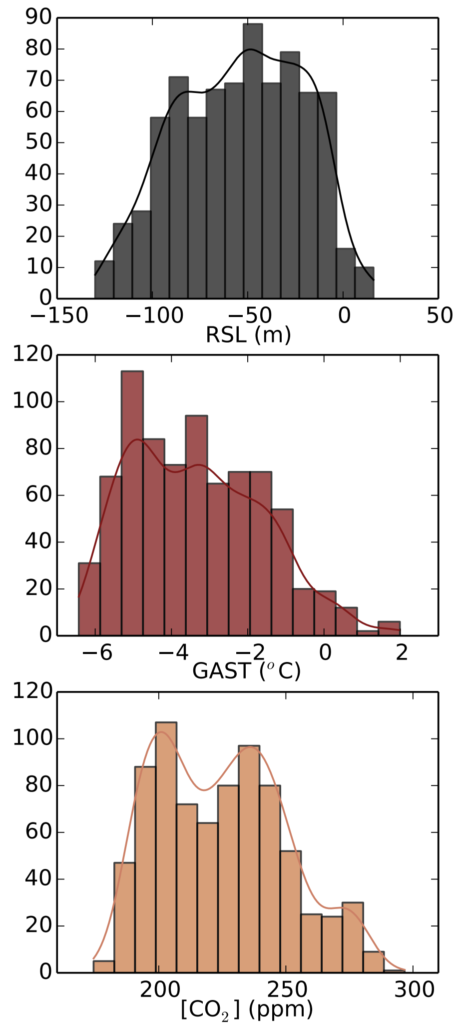

Figure S5. Frequency distributions using the Global Average Surface Temperature reconstruction of Ref. 21. As Figure 2, but replacing δD with GAST.

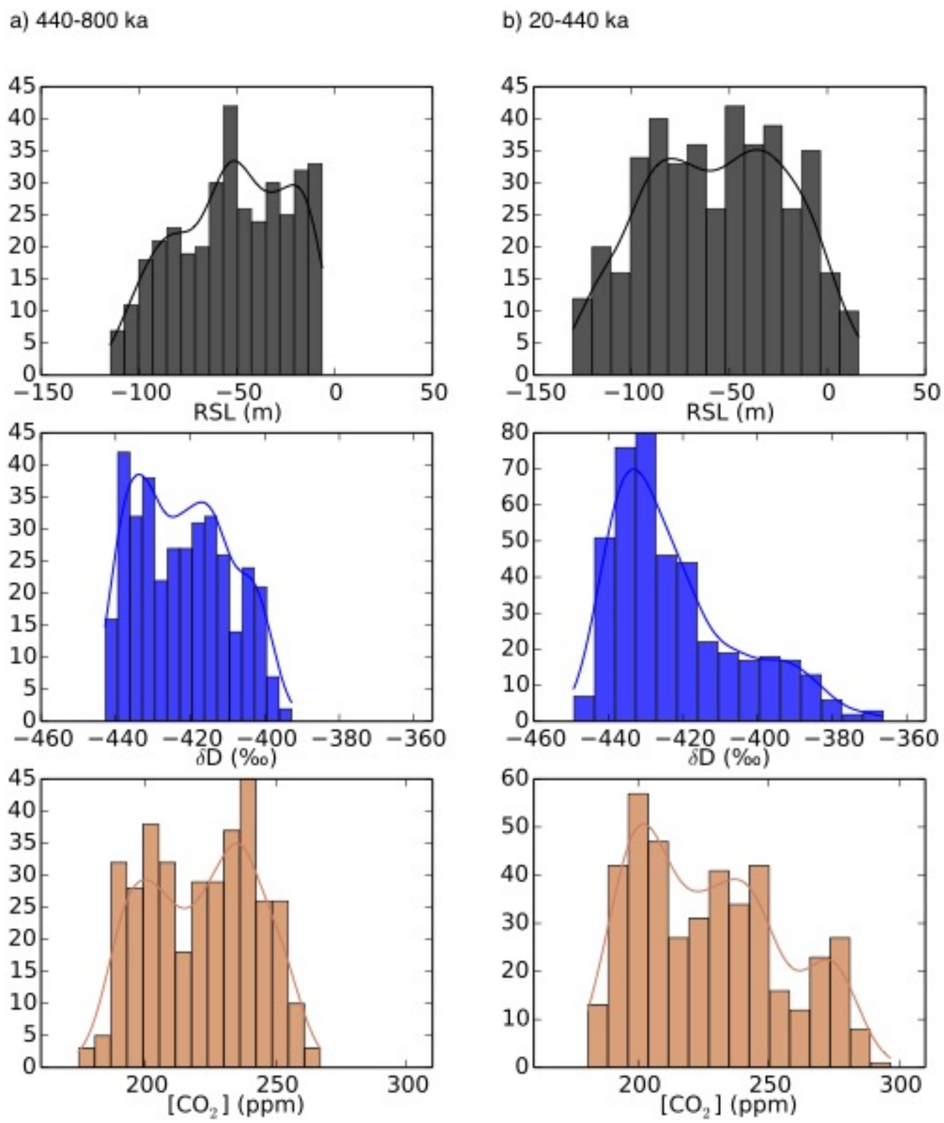

Figure S6. As in Figure 2, showing only (a) 440-800 ka, the lukewarm interglacials and (b) 20-440 ka, the full interglacials.

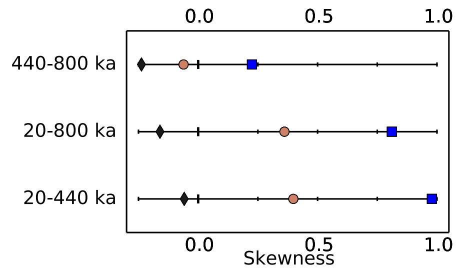

Figure S7. The skewness of the $\delta^{18}O$, EDC δD and atmospheric CO_2 records over (a) 440-800 ka, lukewarm interglacials only, (b) 20-800 ka, the full record considered here, and (c) 20-440 ka, the full interglacials only.

Supplementary References

1 Indermühle, A. *et al.* Holocene carbon-cycle dynamics based on CO_2 trapped in ice at Taylor Dome, Antarctica. *Nature* **398**, 121-126 (1999).

2 Siegenthaler, U. *et al.* Stable Carbon Cycle-Climate Relationship During the Late Pleistocene. *Science* **310**, 1313-1317 (2005).

3 Ahn, J., Brook, E. J. & Howell, K. A high-precision method for measurement of paleoatmospheric CO_2 in small polar ice samples. *Journal of Glaciology* **55**, 499-506 (2009).

4 Lüthi, D. *et al.* High-resolution carbon dioxide concentration record 650,000-800,000 years before present. *Nature* **453**, 379-382 (2008).

5 Barnola, J. M., Raynaud, D., Neftel, A. & Oeschger, H. Comparison of CO_2 measurements by two laboratories on air from bubbles in polar ice. *Nature* **303**, 410-413 (1983).

6 Schmitt, J., Schneider, R. & Fischer, H. A sublimation technique for high-precision measurements of $^{13}CO_2$ and mixing ratios of CO_2 and N_2O from air trapped in ice cores. *Atmos. Meas. Tech.* **4**, 1445-1461 (2011).

7 Lüthi, D. *Hochauflösende CO2 Konzentrationsmessungen an antarktischen Eisbohrkernen: Natürliche Variabilität der letzten 800'000 Jahre und Unsicherheiten aufgrund von Prozessen im Eis* Ph.D. thesis, University of Bern, (2009).

8 Bereiter, B., Stocker, T. F. & Fischer, H. A centrifugal ice microtome for measurements of atmospheric CO_2 on air trapped in polar ice cores. *Atmos. Meas. Tech.* **6**, 251-262 (2013).

9 Smith, H. J., Wahlen, M., Mastoianni, D., Taylor, K. & Mayewski, P. The CO_2 concentration of air trapped in Greenland Ice Sheet Project 2 ice formed during periods of rapid climate change. *Journal of Geophysical Research* **102**, 26,577-526,583 (1997).

10 Tschumi, J. & Stauffer, B. Reconstructing past atmospheric CO_2 concentration based on ice-core analyses: open questions due to in situ production of CO_2 in the ice. *Journal of Glaciology* **46**, 45-53 (2000).
11 Schmitt, J. *et al.* Carbon Isotope Constraints on the Deglacial CO_2 Rise from Ice Cores. *Science* **336**, 711-714 (2012).
12 Schneider, R., Schmitt, J., Köhler, P., Joos, F. & Fischer, H. A reconstruction of atmospheric carbon dioxide and its stable carbon isotopic composition from the penultimate glacial maximum to the last glacial inception. *Clim. Past* **9**, 2507-2523 (2013).
13 Marcott, S. A. *et al.* Centennial-scale changes in the global carbon cycle during the last deglaciation. *Nature* **514**, 616-619 (2014).
14 Lüthi, D. *et al.* CO_2 and O_2/N_2 variations in and just below the bubble-clathrate transformation zone of Antarctic ice cores. *Earth and Planetary Science Letters* **297**, 226-233 (2010).
15 Bereiter, B. *et al.* Mode change of millennial CO_2 variability during the last glacial cycle associated with a bipolar marine carbon seesaw. *Proc Natl Acad Sci USA* **109**, 9755-9760 (2012).
16 Eggleston, S., Schmitt, J., Bereiter, B., Schneider, R. & Fischer, H. Evolution of the stable carbon isotope composition of atmospheric CO_2 over the last glacial cycle. *Paleoceanography* **31**, 434-452 (2016).
17 Masson-Delmotte, V., Stenni, B. & Jouzel, J. Common millennial-scale variability of Antarctic and Southern Ocean temperatures during the past 5000 years reconstructed from the EPICA Dome C ice core. *The Holocene* **14**, 145-151 (2004).
18 Jouzel, J. *et al.* Orbital and Millennial Antarctic Climate Variability over the Past 800,000 Years. *Science* **317**, 793-796 (2007).
19 Stenni, B. *et al.* The deuterium excess records of EPICA Dome C and Dronning Maud Land ice cores (East Antarctica). *Quat. Sci. Rev.* **29**, 146-159 (2010).
20 Noone, D. & Simmods, I. Sea ice control of water isotope transport to Antarctica and implications for ice core interpretation. *Journal of Geophysical Research* **109**, doi:10.1029/2003JD004228 (2004).
21 Snyder, C. W. Evolution of global temperature over the past two million years. *Nature* **538**, 226-228, doi:10.1038/nature19798 (2016).
22 Elderfield, H. *et al.* Evolution of Ocean Temperature and Ice Volume Through the Mid-Pleistocene Climate Transition. *Science* **337**, 704-709 (2012).
23 Shakun, J. D., Lea, D. W., Lisiecki, L. E. & Raymo, M. E. An 800-kyr record of global surface ocean $\delta^{18}O$ and implications for ice volume-temperature coupling. *Earth Planet Sci Lett* **426**, 58-68 (2015).
24 Spratt, R. M. & Lisiecki, L. E. A Late Pleistocene sea level stack. *Clim Past* **12**, 1079-1092 (2016).